

## Optical spectra in (La,Y)TiO<sub>3</sub>: Variation of Mott-Hubbard gap features with change of electron correlation and band filling

Y. Okimoto, T. Katsufuji, Y. Okada, T. Arima, and Y. Tokura  
*Department of Physics, University of Tokyo, Tokyo 113, Japan*  
 (Received 27 July 1994; revised manuscript received 13 January 1995)

Optical spectra have been investigated for the prototypical Mott-Hubbard (MH) insulators LaTiO<sub>3</sub> and YTiO<sub>3</sub>, and their solid solutions La<sub>x</sub>Y<sub>1-x</sub>TiO<sub>3</sub>. The MH gap shows a critical variation with  $x$  or equivalently with the change of the one-electron bandwidth  $W$ . By an extrapolation of the rapidly varying MH gap with the electron correlation strength ( $\tilde{U} = U/W$ ), we could determine the relative distance of each compound from the hypothetical Mott transition point ( $\tilde{U}_c$ ). The band-filling dependence of the gap spectra has been also investigated for LaTiO<sub>3+ $\delta$ /2</sub> with the nominal hole concentration  $\delta$ . The systematic collapse of the MH gap is argued, together with similar results on filling-controlled compounds Y<sub>1-x</sub>Ca<sub>x</sub>TiO<sub>3</sub>, in terms of doping-induced spectral weight transfer.

### I. INTRODUCTION

Electronic properties of transition metal oxide compounds with a strong electron correlation effect have been attracting renewed interest since the advent of extensive studies on the normal state properties of high- $T_c$  superconducting cuprates. In particular, the insulator-to-metal transition with a change of the band filling (or with the so-called carrier-doping procedure) as well as possibly exotic properties of thus deduced metallic states have been central issues in recent studies. Among various transition metal oxides, the perovskite structure  $AMO_3$  ( $A$  being the trivalent or divalent metal ion and  $M$  being the  $3d$  transition metal) is suitable for a systematic study on the insulator-metal transition (Mott transition), since the band filling as well as the strength of the electron correlation can be controlled to some extent by means of elemental substitution on the  $A$  site.<sup>1-3</sup> The purpose of the present paper is to report on the variation of the charge gap features in the prototypical Mott-Hubbard insulators LaTiO<sub>3</sub>, YTiO<sub>3</sub>, and their solid solutions La<sub>x</sub>Y<sub>1-x</sub>TiO<sub>3</sub> with change of the electron correlation strength and the band filling.

The perovskite  $RTiO_3$  ( $R$ =rare earth) and its hole-doped analog  $R_{1-x}A_xTiO_3$  ( $A$ =alkaline-earth) have been proposed as one of the most appropriate systems for experimental investigation on the doping-induced Mott transition.<sup>4-9</sup> The nominal valence of Ti in the end insulators  $RTiO_3$  is  $3+$  with  $3d^1$  ( $s = 1/2$ ) configuration. The crystal structure of  $RTiO_3$  is of the GdFeO<sub>3</sub>-type, in which Ti sites form a quasisimple cubic lattice, yet the TiO<sub>6</sub> octahedra tilt alternately along each orthogonal direction.<sup>10</sup> As a result, the transfer interaction of the  $3d$  electron or the one-electron bandwidth ( $W$ ) shows a considerable variation depending on the tilting angle (i.e., Ti-O-Ti bond angle). This is because the  $3d$  electron transfer in titanium oxides is governed by the supertransfer process mediated by the O  $2p$  states rather than the direct transfer between the  $3d$  states.<sup>11</sup> For ex-

ample, the Ti-O-Ti bond angle ( $= 157^\circ$ ) for LaTiO<sub>3</sub> is decreased to  $140^\circ$  with full substitution of La-site with Y (i.e., YTiO<sub>3</sub>),<sup>10</sup> which may cause the reduction of the  $3d t_{2g}$  electron bandwidth ( $W$ ) as much as 30% as argued in the following section. Thus, with use of the solid solution systems La<sub>x</sub>Y<sub>1-x</sub>TiO<sub>3</sub> in which the lattice parameters vary continuously with  $x$ , the  $W$  value can be controlled. LaTiO<sub>3</sub> has been recently proved to be located in the immediate vicinity of the insulator-metal boundary.<sup>4,5,8,9</sup> In fact, we demonstrate below that the Mott-Hubbard gap increases with the Y concentration ( $1-x$ ) or equivalently with an increase of the electron correlation.

Another advantage of utilizing the present titanate systems for the investigation on the Mott transition is that the band filling can be controlled as well with substitution of  $R$ -site with divalent alkaline-earth ions or with introducing extra oxygen. In particular, the end insulator LaTiO<sub>3</sub>, with a relatively small Mott-Hubbard gap ( $\sim 0.2$  eV) can be metallized by introducing about 1% of nonstoichiometric oxygen.<sup>8</sup> We may spectroscopically investigate the change of the electronic structure or the collapse of the Mott-Hubbard gap in the course of the Mott transition caused by such hole doping. Thus, the compositional control of the perovskite titanates enables one to investigate the critical changes of electronic properties on the verge of the metal-correlated insulator phase boundary as a function of the both parameters, i.e., the correlation strength and the band filling.

### II. EXPERIMENT

#### A. Sample preparation and characterization

All the samples were melt grown by a floating-zone method. Starting materials were Ti, TiO<sub>2</sub>, La<sub>2</sub>O<sub>3</sub>, and Y<sub>2</sub>O<sub>3</sub>. The powder of TiO<sub>2</sub>, La<sub>2</sub>O<sub>3</sub>, and Y<sub>2</sub>O<sub>3</sub> was well dried by firing them at 1000 °C in air before use.

For preparation of the mixed crystal (solid solution) of  $\text{La}_x\text{Y}_{1-x}\text{TiO}_3$ , respective raw materials were weighed to a prescribed ratio of  $\text{La}_x\text{Y}_{1-x}\text{TiO}_{2.94}$  and the mixture was pressed into two rods (5 mm  $\phi \times 20$  mm and 5 mm  $\phi \times 100$  mm). These bars were loaded in a floating-zone furnace equipped with two halogen incandescent lamps and double hemielliptic mirrors. For the growth of  $\text{La}_x\text{Y}_{1-x}\text{TiO}_3$  ( $0 \leq x \leq 1$ ), the ingredient was melted in a reducing atmosphere by flowing mixed gas of  $\text{H}_2/\text{Ar}$ .

It has become known by recent experimental investigations<sup>8</sup> that electronic properties of  $\text{LaTiO}_3$  is extremely sensitive to slight nonstoichiometry of oxygen. This is because  $\text{LaTiO}_3$  locates on the verge of Mott transition and even a small amount of "holes" introduced by excess oxygen drive the insulator-metal transition. In other words, we can finely control the band filling ( $n = 1 - \delta$ ) by preparing slightly off-stoichiometric samples of  $\text{LaTiO}_{3+\delta/2}$ , which can be grown in an atmosphere of various reducing conditions with use of gas mixture of  $\text{Ar}/\text{H}_2$ . The oxygen off-stoichiometry ( $\delta/2$ ) was determined by thermogravimetric analysis for  $\text{LaTiO}_3$  and  $\text{YTiO}_3$ .  $\text{LaTiO}_{3+\delta/2}$  samples with  $\delta = 0.08, 0.05, 0.04, 0.02$ , and  $0.01$  could be grown in an atmosphere of  $\text{H}_2/\text{Ar}$  mixture with the ratio of 7%, 15%, 17%, 19%, and 30%  $\text{H}_2/\text{Ar}$ , respectively. The crystal of  $\text{YTiO}_3$ , which was grown in a fairly strong reducing condition (30%  $\text{H}_2/\text{Ar}$ ), shows the stoichiometry of  $\text{YTiO}_{3.01}$  ( $\delta = 0.02$ ). All other samples of the solid solutions  $\text{La}_x\text{Y}_{1-x}\text{TiO}_3$  were melt grown in a similarly strong reducing atmosphere (30%  $\text{H}_2/\text{Ar}$ ). We have not done the TGA measurements on these samples, yet the oxygen off-stoichiometry ( $\delta/2$ ) is perhaps less than 0.01 judging from the results for  $\text{LaTiO}_3$  and  $\text{YTiO}_3$ .

Measurements of powder x-ray diffraction patterns showed that the obtained samples were of a single phase. The crystal structure was perovskitelike with an orthorhombic distortion (i.e., of  $\text{GdFeO}_3$ -type structure), over the whole concentration of  $x$ . To characterize the compounds, we have measured temperature dependence of resistivity and magnetic susceptibility. For the resistivity measurements, the samples were cut to a rectangular shape and the four-probe contacts were made with indium. Magnetic susceptibility was measured with a superconducting quantum interference device magnetometer. To determine a critical temperature for the ferromagnetic or weakly ferromagnetic (spin canted) phase transition, we also measured the temperature dependence of the field-cooled magnetization with the application of a relatively weak magnetic field (10 mT).

Apart from the intentionally oxygen-doped samples of  $\text{LaTiO}_{3+\delta/2}$  ( $\delta \geq 0.02$ ) prepared in a weakened reducing atmosphere, all the compounds show electrically insulating or semiconducting behavior with room temperature resistivity of above  $0.5 \Omega \text{ cm}$ . As for the resistivity of  $\text{LaTiO}_{3+\delta/2}$ , the resistivity value and its temperature dependence were observed to be critically dependent on the nominal hole concentration  $\delta$ , which is described in detail in the latter section.

We show in Fig. 1 the  $x$ -dependent variation of the magnetic transition temperatures for the presently obtained samples  $\text{La}_x\text{Y}_{1-x}\text{TiO}_3$  in comparison with the

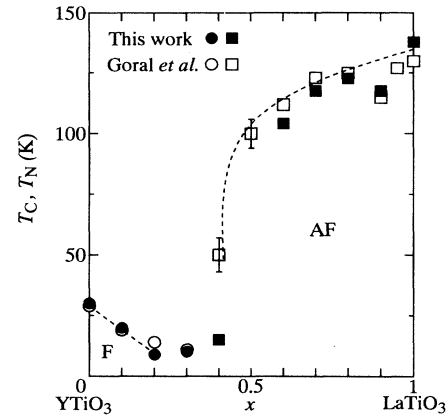


FIG. 1. Magnetic phase transition temperatures ( $T_C$  and  $T_N$ ) for  $\text{La}_x\text{Y}_{1-x}\text{TiO}_3$ ;  $F$  and  $AF$  stand for the ferromagnetic and antiferromagnetic ordering. The  $AF$  phase is weakly ferromagnetic with spin canting.

data reported previously by Goral *et al.*<sup>12</sup> In spite of different procedures of preparing the samples, i.e., the floating-zone method in a 30%  $\text{H}_2/\text{Ar}$  gas atmosphere in the present case and an arc-melting method in  $\text{Ar}$  atmosphere in their study, the agreement between the both results is fairly good. The  $\text{La}$ -rich samples with  $x \geq 0.4$  show a weak ferromagnetism due to canting of antiferromagnetically ordered  $s = 1/2$  spins, while the  $\text{Y}$ -rich samples with  $x \leq 0.2$  show the well-defined ferromagnetic ground state. Around  $x = 0.3$ , the magnetic susceptibility obeys approximately Curie law, indicating mutual compensation of antiferromagnetic and ferromagnetic exchange interaction. Such a *ferromagnetic* Mott insulator arises perhaps from the orbital (pseudo)degeneracy

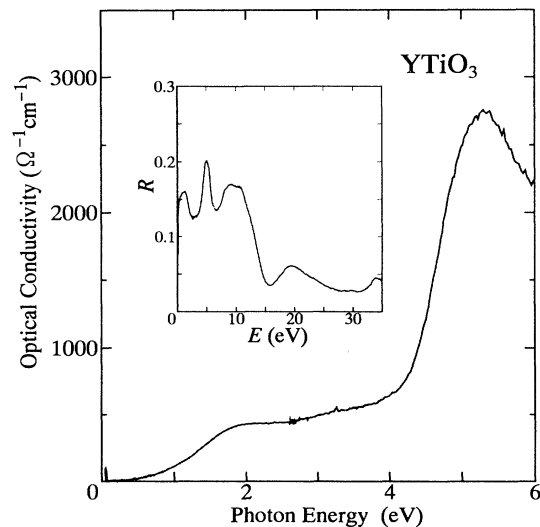


FIG. 2. Spectrum of optical conductivity in  $\text{YTiO}_3$  in an extended energy region up to 6 eV at room temperature. Rises of the optical conductivity around 1 and 4 eV correspond to the onsets of the Mott-Hubbard gap and charge-transfer gap transitions, respectively. The inset shows the reflectivity spectrum up to 35 eV.

of  $t_{2g}$ -like states. The sign of the exchange interaction between neighboring Ti spins may be governed by the Ti-O-Ti bond angle and the smaller bond angle in Y-rich (lower  $x$ ) samples may favor the ferromagnetic exchange interaction. Otherwise, the ferromagnetism present in the Y-rich compounds with a reduced one-electron bandwidth ( $W$ ) may be characteristic of the orbital ordered ferromagnetism, which can be described by the degenerate (multiband) Hubbard model.<sup>13-15</sup> We will not discuss this unsettled problem of the magnetic phase diagram of  $\text{La}_x\text{Y}_{1-x}\text{TiO}_3$  and  $R\text{TiO}_3$  (Refs. 4, 12, 16, and 17) ( $R$  ranging over whole rare earth elements except for divalent Eu) any further here, though the magnetic ordering effect might have to be properly taken into account for the low-temperature optical spectra.

### B. Measurements of optical reflectivity

The reflectivity spectra were measured at room temperature in the energy range of 0.05 eV–40 eV, using a Fourier-transform interferometer (0.05 eV–0.8 eV) and a grating monochromator (0.6 eV–40 eV). For the vacuum ultraviolet region, synchrotron radiation (INS-SOR) at Institute for Solid State Physics, University of Tokyo was utilized. All the samples were specularly polished with alumina powder and the reflectivity was measured in the condition of nearly normal incidence. To derive spectra of optical conductivity, Kramers-Kronig analysis was performed on the reflectivity data. For this purpose, we extrapolated the reflectivity data such that the reflectivity is constant below 0.05 eV and varies as  $\propto 1/\omega^4$  above 40 eV.

## III. VARIATION OF MOTT-HUBBARD GAP WITH CHANGE OF ONE-ELECTRON BANDWIDTH

### A. Optical conductivity spectra of the Mott-Hubbard gap in $\text{La}_x\text{Y}_{1-x}\text{TiO}_3$

To overview the electronic gap features in these  $\text{Ti}^{3+}$ -based oxide compounds, we first show in Fig. 2 reflectivity spectrum up to 35 eV (inset), as well as the deduced optical conductivity spectrum for  $\text{YTiO}_3$  up to 6 eV. Two gaplike features are clearly discernible around 1 eV and 4 eV as distinct rises in the optical conductivity spectrum. (A sharp spike below 0.1 eV is due to an optical phonon mode.) These features can be interpreted as the Mott-Hubbard gap transition between the lower and upper Hubbard bands of  $t_{2g}$ -like character and the charge-transfer type gap transition from the O  $2p$  states to the upper Hubbard  $3d$  band, respectively.<sup>18</sup> Hereafter, we focus on the lower-lying Mott-Hubbard (MH) gap structure, which is sensitive to electronic parameters like the one-electron bandwidth ( $W$ ).

A variation in reflectivity spectra in the MH gap region is shown in Fig. 3 for  $\text{La}_x\text{Y}_{1-x}\text{TiO}_3$ . The reflectivity band at 1–2 eV is observed to shift to lower energy with increasing La concentration ( $x$ ). For the  $x = 1$  sample,

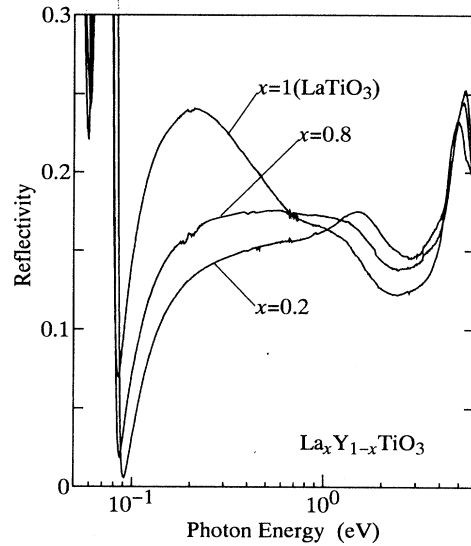


FIG. 3. Spectra of reflectivity in  $\text{La}_x\text{Y}_{1-x}\text{TiO}_3$  at room temperature.

we observe an additional bump structure at  $\sim 0.2$  eV. This can be ascribed to the presence of a small amount of charge carrier in  $\text{LaTiO}_{3+\delta/2}$  sample with  $\delta = 0.01$  (*vide infra*). We show in Fig. 4 the optical conductivity spectra for the MH gaps, which were deduced by Kramers-Kronig transformation of the respective reflectivity data. As clearly seen in the figure, the onset of the optical conductivity shifts to lower energy with increasing  $x$ , indicating a continuous change of the MH gap with  $x$ . A similarly systematic change of the MH gap spectra for the perovskite Ti oxides was also reported on  $R\text{TiO}_3$  with varying the  $R$  site ( $R = \text{La}, \text{Ce}, \text{Nd}, \text{Sm}, \text{and Gd}$ ) by Crandles *et al.*<sup>3</sup> They have observed the increase of the Mott gap with increasing the  $R$ -site ion radius, which may correspond to a decrease of  $x$  in the present  $\text{La}_x\text{Y}_{1-x}\text{TiO}_3$  system.

In  $\text{La}_x\text{Y}_{1-x}\text{TiO}_3$ , however, we have observed some nonsystematic behaviors in the  $x$ -dependent change of

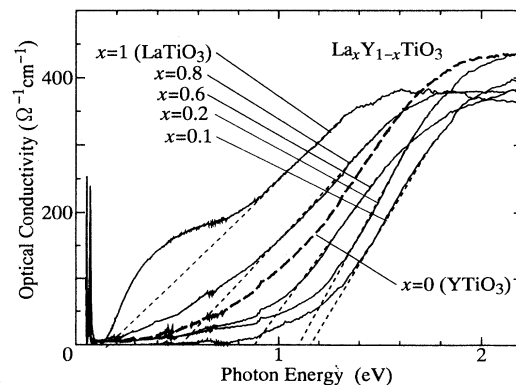


FIG. 4. Spectra of optical conductivity in  $\text{La}_x\text{Y}_{1-x}\text{TiO}_3$  at room temperature. A crossing point of a baseline and a dashed line is defined as the Mott-Hubbard gap energy.

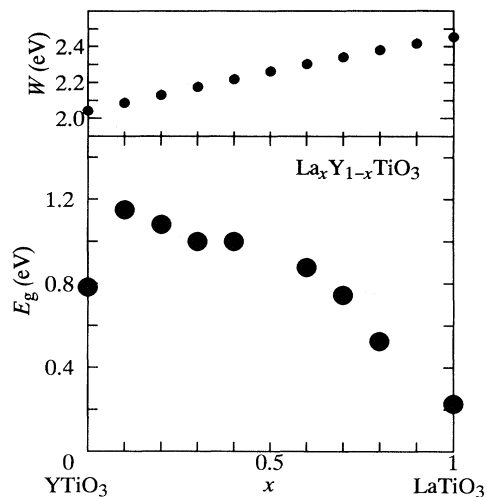


FIG. 5. The Mott-Hubbard gap energies in  $\text{La}_x\text{Y}_{1-x}\text{TiO}_3$  as determined by the onsets of the optical conductivity (Fig. 4). The upper panel shows a variation of the one-electron bandwidth calculated by a tight binding model (see text).

the optical conductivity spectra: A spectrum of  $\text{YTiO}_3$  (shown in Fig. 4 by a broken curve) appears to be positioned between the  $x = 0.6$  and  $x = 0.8$  spectrum and violates the systematic trend of the spectral position from  $x = 0$  up to  $x = 0.9$ . Another problem is an additional shoulder structure around 0.1 eV, observed only in the spectrum of  $\text{LaTiO}_3$ , which corresponds to the reflectivity bump at 0.2 eV (see Fig. 3). As demonstrated later by using experimental results with a varying oxygen content, this structure is ascribable to the presence of extra carriers arising from slight nonstoichiometry ( $\delta = 0.01$ ) of oxygen in the sample of  $\text{LaTiO}_{3+\delta/2}$ . The sample of  $\text{LaTiO}_3$  used in the measurement for Fig. 4 is the most reduced, i.e., the most stoichiometric one among those we prepared. Nevertheless, even a small deviation of the band filling ( $n = 1 - \delta$ ) thus causes an appreciable deformation in the gap spectra, perhaps due to the relatively weak correlation effect (i.e., a small MH gap) in  $\text{LaTiO}_3$ . Judging from the reflectivity value and the spectral shape, as well as the temperature dependence of the resistivity, the spectra which have been reported so far for  $\text{LaTiO}_3$  (Refs. 3, 6, and 9) appears to be for less stoichiometric (i.e., more conducting) than the present one and hence more seriously affected by the presence of extra holes.

We have estimated the true onset of the MH gap transition by extrapolating the spectral feature from the higher-energy side as indicated by dashed lines in Fig. 4. Thus derived MH gap energy ( $E_g$ ) for  $\text{La}_x\text{Y}_{1-x}\text{TiO}_3$  is plotted as a function of  $x$  in Fig. 5. Apart from the  $x = 0$  compound  $\text{YTiO}_3$ , the MH gap energy continuously decreases with  $x$ . The result clearly indicates that the electron correlation effect becomes weaker with increasing La concentration ( $x$ ). The change of electron correlation strength apparently originates from a change in the  $3d$  electron hopping interaction or the one-electron bandwidth ( $W$ ), which is governed by the change of Ti-

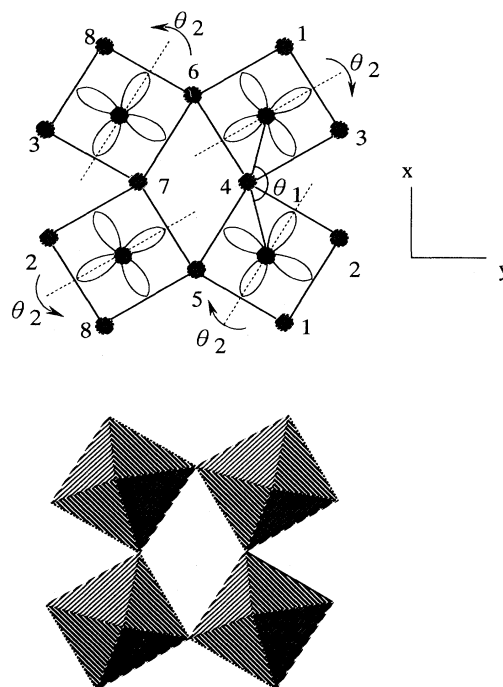


FIG. 6. Arrangement ( $xy$  plane) of the  $\text{TiO}_6$  octahedra in the orthorhombically distorted perovskite lattice, which is taken into account for the calculation of the  $t_{2g}$ -like band dispersion (see text).

O-Ti bond angle as demonstrated by the calculation in the next section. Concerning the deviation of the MH gap ( $E_g$ ) of  $\text{YTiO}_3$  from the systematic tendency, we have no definite explanation for this at present, yet can speculate the following two possible origins: The seemingly most probable cause would be the presence of an appreciable amount of carriers arising from the oxygen nonstoichiometry in  $\text{YTiO}_3$ . Such carriers would cause a shift of the gap or at least a spectral weight transfer to lower energy as discussed in detail in the latter section. However, our thermogravimetric analysis indicates that the sample used in the present study shows a stoichiometry of  $\text{YTiO}_{3.01}$  ( $\delta = 0.02$ ) and ferromagnetic phase transition at 30 K, typical of a well-stoichiometric sample. We have also investigated the spectrum of a less stoichiometric sample  $\text{YTiO}_{3+\delta/2}$  with  $\delta = 0.06$  and reduced  $T_c$  of 25 K, but observed essentially no appreciable change of the spectral onset within such a small variation of the filling. Therefore, the sudden decrease of the MH gap can be hardly ascribable to the sample nonstoichiometry. Another possible origin of the nonsystematic small gap for  $\text{YTiO}_3$  may be ascribed to the orbital ordering effect characteristic of the degenerate Hubbard system with the ferromagnetic ground state.<sup>13-15</sup> When the orbital of  $t_{2g}$  electrons on the neighboring Ti sites are of different characters, e.g.,  $d_{zx}$  vs  $d_{yz}$ , the final state of the optical transition accompanies the  $3d$ -electron vacant state on one Ti site and two  $t_{2g}$  electrons with parallel spins on the other Ti site. Then, the Hund coupling or intra-atomic exchange interaction may consider-

ably reduce the gap energy. Such a situation has been, in fact, observed in the systematic optical study on the electron-correlation gaps for LaMO<sub>3</sub> ( $M$  being all the 3d transition metal element).<sup>18</sup> In order to confirm the latter hypothesis, further studies such as polarized neutron scattering measurements would be needed.

### B. Systematics for the Mott-Hubbard gap with change of correlation strength

The substitution of La sites with Y of a smaller ionic radius causes an increase of orthorhombic distortion in perovskite-like lattice and a resultant decrease of the one-electron band width as quantitatively demonstrated in the following. The pattern of the distortion is the alternating tilting of the TiO<sub>6</sub> octahedra along the respective  $x$ ,  $y$ , and  $z$  directions of the primitive cubic lattice of the perovskite. The bond angles for LaTiO<sub>3</sub> are 157° in the  $ab$  plane and 158° along the  $c$  axis, while those for YTiO<sub>3</sub> are 140° and 144°, respectively. The Ti-O-Ti bond angle bears a close relationship with the lattice parameters of the GdFeO<sub>3</sub>-type orthorhombic cell,  $a$ ,  $b$ , and  $c$ , which are approximately  $\sqrt{2}a_p$ ,  $\sqrt{2}a_p$ , and  $2a_p$ , respectively,  $a_p$  being the unit cell parameter of the cubic perovskite. This has been confirmed by MacLean, Ng, and Greedan<sup>10</sup> for various RTiO<sub>3</sub> crystals and also related GdFeO<sub>3</sub>-type structures. Therefore, we may accurately interpolate the Ti-O-Ti bond angle ( $\theta$ ) in the solid solution La <sub>$x$</sub> Y<sub>1- $x$</sub> TiO<sub>3</sub> with use of the measured lattice parameters. Substantially,  $\theta$  varies almost linearly with  $x$  between the both end compounds.

The bond angle deviation from 180° reduces the effective  $d$  electron hopping interaction, since the  $d$  electron transfer is dominated by the supertransfer interaction via the O  $2p$  states rather than the direct  $d$ - $d$  hopping.<sup>11</sup> Here, we should note that the 3d orbitals split into two levels,  $t_{2g}$ -like and  $e_g$ -like states, due to the crystal field effect. The real crystal of RTiO<sub>3</sub> shows the orthorhombic distortion deviating from the point group symmetry of O <sub>$h$</sub>  and hence the degeneracy of  $t_{2g}$  is lifted more or less. However, such a splitting of the  $t_{2g}$ -like orbitals may be neglected as compared with the magnitude of the 3d one-electron bandwidth ( $> 1$  eV) and of the intra-atomic exchange interaction (Hund coupling energy): The right octahedral shape of the TiO<sub>6</sub> unit is least deformed even in the orthorhombically distorted lattice structure<sup>10</sup> and hence the ligand field is minimally affected.

Then, let us consider the  $d$  electron band dispersion with the use of the tight binding model in the presence of the bond angle distortion. A similar consideration has been already attempted by Crandles *et al.*<sup>3</sup> for the change in the bandwidth for the distorted RTiO<sub>3</sub> ( $R = \text{La, Ce, Pr, Nd, Sm, and Gd}$ ). However, their calculation was done on the simplified lattice structure model and with an inappropriate set of base functions ( $4 \times 4$  Hamiltonian matrix) with neglect of the crystal field effect, which appears to result in an exaggerated dependence of the band dispersion on the bond angle distortion. To improve this estimation, we have adopted the following approach: To deduce the  $t_{2g}$ -like band dispersion, we have

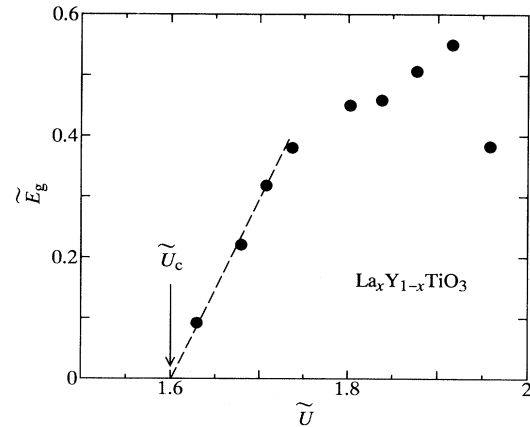


FIG. 7. Normalized gap energy  $\tilde{E}_g (= E_g/W)$  vs correlation strength  $\tilde{U} (= U/W)$  for La <sub>$x$</sub> Y<sub>1- $x$</sub> TiO<sub>3</sub>. The one-electron bandwidth  $W$  for each compound is calculated by the tight binding model (see the upper panel of Fig. 5 and text). The arrow labeled  $\tilde{U}_c$  indicates the critical value of  $\tilde{U}$  for the hypothetical Mott transition, which is extrapolated as shown by a dashed line.

diagonalized the  $28 \times 28$  Hamiltonian matrix with use of Harrison's parametrization<sup>11</sup>. The set of base functions consists of four Ti  $3d$   $t_{2g}$  and twenty-four O  $2p$  orbitals (three orbitals  $\times$  eight sites) as depicted in Fig. 6, which are used to retain the translational symmetry of the orthorhombic lattice. The local rotation angles of the TiO<sub>6</sub> octahedra are denoted as  $\theta_1$  and  $\theta_2$  in Fig. 6, and deduced from the crystallographic data.<sup>10</sup> Here, we have adopted the strong ligand field approximation and neglected the mixing between the O  $2p$  orbitals.

By this procedure, we have obtained the  $d_{xy}$  band dispersion. For example, the dispersion width between the  $\Gamma$ - $X$  points is calculated such as 1.45 eV for LaTiO<sub>3</sub> and 1.17 eV for YTiO<sub>3</sub>, which should replace the values (0.99 eV for LaTiO<sub>3</sub> and 0.46 eV for YTiO<sub>3</sub>) reported previously.<sup>3</sup> Such a large difference mainly comes from taking the crystal field effect into account. The band dispersion is the largest along the  $\Gamma$ - $R$  direction [i.e.,  $(\pi, \pi, \pi)$  direction] in the pseudocubic lattice. ( $d_{xy}$ ,  $d_{yz}$ , and  $d_{zx}$  band are degenerated in this direction.) We show in the upper panel of Fig. 5 thus obtained  $W$  values (i.e., the dispersion along the  $\Gamma$ - $R$  direction) as a function of  $x$  in La <sub>$x$</sub> Y<sub>1- $x$</sub> TiO<sub>3</sub>. The present result shows that the calculated bandwidth  $W$  gradually reduces from 2.45 eV for LaTiO<sub>3</sub> to 2.04 eV for YTiO<sub>3</sub> with decrease of  $x$ .

We redraw the MH gap systematics in Fig. 7 by scaling the data with  $W$ . We plot the normalized MH gap,  $\tilde{E}_g = E_g/W$ , against the electron correlation magnitude  $\tilde{U} = U/W$  for the respective compounds. Here, the on-site Coulomb repulsion energy  $U$  (Hubbard  $U$  term) is tentatively assumed as a constant ( $U = 4$  eV) irrespective of the composition  $x$  by referring to the analysis of photoemission data on Ti<sup>3+</sup>-based oxides.<sup>19</sup> In this sense, the scale of the abscissa in Fig. 7 should not be taken as rigorously quantitative and merely stands for the  $x$ -dependent variation of the electron correlation effect in

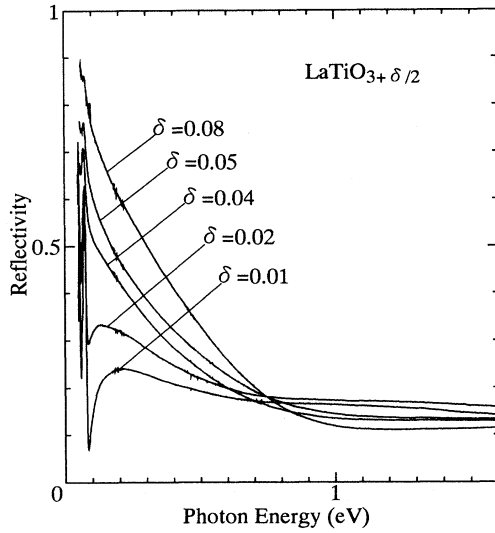


FIG. 8. Spectra of reflectivity in  $\text{LaTiO}_{3+\delta/2}$  at room temperature.

somewhat arbitrary scale.

As clearly seen in Fig. 7, the  $\tilde{E}_g$  value for  $\text{La}_x\text{Y}_{1-x}\text{TiO}_3$  shows a large variation (0.1–0.6) in the relatively narrow range of  $\tilde{U}$  (1.6–1.9). In particular, the  $\text{LaTiO}_3$  (the most left point in Fig. 7) seems to locate on the verge of the gap closure as judged from the critical change of the MH gap in La-rich region, though the most insulating (best stoichiometric)  $\text{LaTiO}_3$  ( $\delta = 0.01$ ) cannot be metallized by application of pressure at least up to 2 GPa.<sup>8</sup> With the extrapolation of the  $\tilde{E}_g$  vs  $\tilde{U}$  plot as indicated by a dashed line, we may tentatively estimate the critical value  $\tilde{U}_c$  ( $\sim 1.6$ ), at which the system is supposed to undergo the metal-insulator transition (bandwidth-control Mott transition). In the spirit of the Brinkman-Rice theory,<sup>20</sup> we define the distance from the  $M$ - $I$  boundary for the respective compounds such as  $\eta = \tilde{U}/\tilde{U}_c - 1$ . For the present system, the  $\eta$  value is fairly small, changing from 0.02 ( $\text{LaTiO}_3$ ) to 0.22 ( $\text{YTiO}_3$ ). (Note that the  $\eta$  value is not affected by choice of the  $U$  value.)

#### IV. HOLE-DOPING INDUCED CHANGE OF OPTICAL CONDUCTIVITY SPECTRA

##### A. Optical conductivity spectra in $\text{LaTiO}_{3+\delta/2}$

As mentioned above, the optical spectrum of  $\text{LaTiO}_{3+\delta/2}$  in the MH gap region is significantly affected by a small amount of oxygen off-stoichiometry  $\delta/2$ . This can be attributed to the change of the low-lying electronic structure, due to the deviation of the filling ( $n = 1 - \delta$ ), which tends to drive the compound to the metallic state. The reason why such an effect of the oxygen nonstoichiometry is most significantly observed in  $\text{LaTiO}_3$  and much less in  $\text{YTiO}_3$  is attributed to the magnitude of the MH gap in the original ( $\delta = 0$ ) compounds or equivalently to the strength of the electron

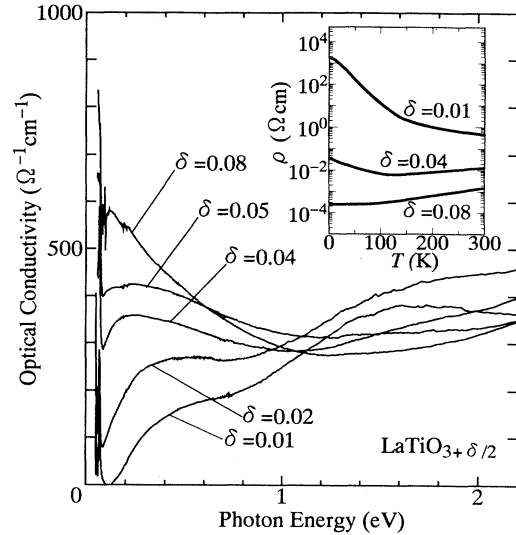


FIG. 9. Spectra of optical conductivity in  $\text{LaTiO}_{3+\delta/2}$  at room temperature. Inset shows temperature dependence of the resistivity for some samples.

correlation as demonstrated in the following.

Let us first discuss the change of the reflectivity spectra for  $\text{LaTiO}_{3+\delta/2}$  (Fig. 8), with variation of  $\delta$ . A bump structure around 0.2 eV in the most stoichiometric compound ( $\delta = 0.01$ ) gradually grows and shifts to lower energy with  $\delta$  and eventually turns into the Drude-like reflectivity band. In accord with this change, a sharp reflectivity structure (0.06 eV) of the oxygen phonon mode fades away due to the dielectric screening effect. For reference, we show in the inset of Fig. 9 temperature dependence of resistivity for some of the crystals whose optical conductivity spectra are shown. The sample with  $\delta = 0.01$  shows an insulating behavior over the whole temperature region, while the  $\delta = 0.08$  sample is metallic. The  $\delta = 0.04$  sample shows a marginal behavior: The resistivity ( $\rho$ ) shows a metallic behavior ( $d\rho/dT \geq 0$ ) at higher temperature, but upturns below around 100 K. A previous study on the similarly processed sample has proved that the inflection point of  $\rho(T)$  coincides with the magnetic transition temperature.<sup>8</sup>

In between  $\delta = 0.01$  and  $\delta = 0.05$ , the change of the conductivity spectra shows an approximately isosbetic point around 1.1 eV as shown in Fig. 9, indicating the one-to-one spectral weight transfer from the MH gap transitions to the inner-gap excitations. This also indicates that the nominal hole-doping collapses the MH gap and evolves the inner-gap states (incoherent states), which eventually turn into the Drude-like states (coherent states) near the Fermi level. Spectroscopically, the growth rate of the sum of the inner-gap states or the destruction rate of the MH gap with hole doping can be measured by such a transferred spectral weight, which is discussed in the following in comparison with the case of  $\text{Y}_{1-x}\text{Ca}_x\text{TiO}_3$  showing a narrower one-electron bandwidth ( $W$ ).

### B. Dependence of spectral weight transfer on strength of electron correlation

The spectral weight transfer from the correlation gap excitations to the inner-gap excitations with a change of the band filling is commonly observed in the carrier-doped correlated insulators, for example in all the cuprate superconductors, perovskite-like Ti, V, and Co oxides.<sup>6,7,21–25</sup> Recent numerical calculations on doped Hubbard clusters have simulated such a phenomenon.<sup>26</sup> For the present titanates systems, we will argue the dependence of the doping-induced electronic structural change on the relative strength of the electron correlation.

In Fig. 10, we compare the doping-induced changes of the optical conductivity spectra for (a) LaTiO<sub>3+δ/2</sub> (and La<sub>1-x</sub>Sr<sub>x</sub>TiO<sub>3</sub>) and (b) Y<sub>1-x</sub>Ca<sub>x</sub>TiO<sub>3</sub>, the latter of which was reproduced from the literature.<sup>7</sup> The spectra of the respective samples are indicated by the value of the band filling ( $n$ ) ( $n = 1 - \delta$  or  $n = 1 - x$ ). Figure 10(a) also includes the spectrum of La<sub>1-x</sub>Sr<sub>x</sub>TiO<sub>3</sub> with  $x = 0.1$  ( $n = 0.9$ ). Spectral changes with  $n$  in the doped LaTiO<sub>3+δ/2</sub> (and La<sub>1-x</sub>Sr<sub>x</sub>TiO<sub>3</sub>) and Y<sub>1-x</sub>Ca<sub>x</sub>TiO<sub>3</sub> fairly resemble each other although the changing rate differs significantly in the respective compounds.

In order to estimate the rate of the spectral weight transfer, we have calculated effective number of electrons ( $N_{\text{eff}}$ ), which is defined as

$$N_{\text{eff}}(\omega_c) = \frac{2m}{\pi e^2 N} \int_0^{\omega_c} \sigma(\omega) d\omega. \quad (1)$$

Here,  $N$  represents the number of the Ti in unit volume. The cutoff energy ( $E_c = \hbar\omega_c$ ) adopted for the estimation of the contribution from the inner-gap excitations is 1.1 eV for LaTiO<sub>3+δ/2</sub> and La<sub>1-x</sub>Sr<sub>x</sub>TiO<sub>3</sub> and 1.6 eV for Y<sub>1-x</sub>Ca<sub>x</sub>TiO<sub>3</sub>, which corresponds to the energies of the approximately isosbetic points of the conductivity spectra (indicated by arrows in Fig. 10) in the low-doped

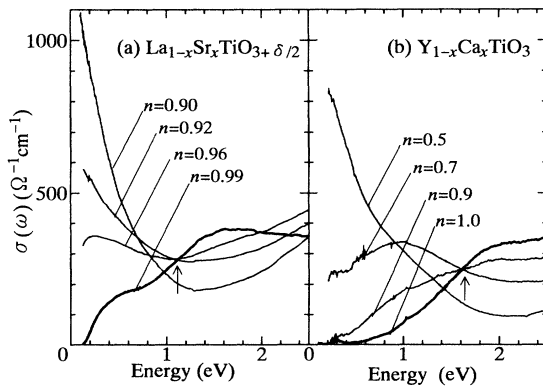


FIG. 10. Optical conductivity spectra of carrier-doped perovskite titanates, (a) LaTiO<sub>3+δ/2</sub> and La<sub>1-x</sub>Sr<sub>x</sub>TiO<sub>3</sub> and (b) Y<sub>1-x</sub>Ca<sub>x</sub>TiO<sub>3</sub>, with a change of the band filling  $n$  ( $n = 1 - x$  or  $1 - \delta$ ). Arrows indicate the isosbetic points in the low-doped regions (see text).

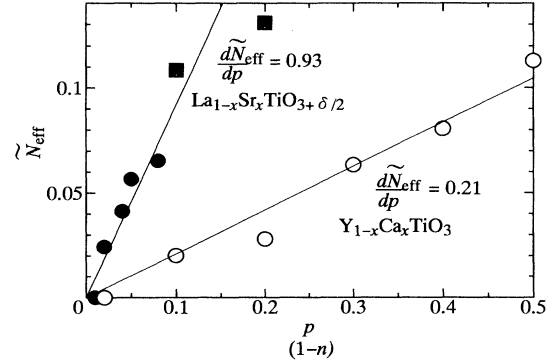


FIG. 11. The hole-concentration  $p$  ( $= \delta$  or  $1 - x$ ) dependence of the effective number of electrons ( $\tilde{N}_{\text{eff}}$ ) in LaTiO<sub>3+δ/2</sub> at 1.1 eV and Y<sub>1-x</sub>Ca<sub>x</sub>TiO<sub>3</sub> at 1.6 eV (see text).

region. Plotted in Fig. 11 is the value of  $\tilde{N}_{\text{eff}}$ , which is defined as subtracted by the value of the respective parent insulator LaTiO<sub>3</sub> (actually LaTiO<sub>0.005</sub>) and YTiO<sub>3</sub>. The slope of the  $\tilde{N}_{\text{eff}}$  against the nominal hole concentration  $p$  ( $p = 1 - n$ , i.e.,  $\delta$  or  $x$ ) differs significantly for the two systems;  $d\tilde{N}_{\text{eff}}/dp \sim 0.9$  and  $\sim 0.2$  for the doped LaTiO<sub>3</sub> and YTiO<sub>3</sub> system, respectively. Such a large difference may be attributed to the difference in strength of the electron correlation, which manifests itself in the distance from the Mott transition point,  $\eta$  ( $= \tilde{U}/\tilde{U}_c - 1$ );  $\eta = 0.02$  for LaTiO<sub>3</sub> and  $\eta = 0.22$  for YTiO<sub>3</sub>. In other words, the MH gap feature is more amenable to the change of the band filling (or carrier-doping) for the compound with weaker electron correlations (a smaller  $\eta$  value). For the test of this idea, further experimental investigation of the  $\eta$  dependence of  $d\tilde{N}_{\text{eff}}/dp$  is needed, using the present titanate systems with control of both the band filling and correlation strength.

It is also interesting to compare the transfer rate of the titanates with those of the doped cuprate compounds.<sup>21–23</sup> For example, the corresponding slope in the  $\tilde{N}_{\text{eff}}$  vs  $p$  plot in La<sub>2-x</sub>Sr<sub>x</sub>CuO<sub>4</sub> was reported to be  $\sim 1.6$ ,<sup>21</sup> which is even larger than that of the doped LaTiO<sub>3</sub> system ( $\sim 0.9$ ), in spite of the much larger charge gap in La<sub>2</sub>CuO<sub>4</sub> ( $\sim 1.5$  eV) than in LaTiO<sub>3</sub> ( $\sim 0.2$  eV). Such a different behavior of the spectral weight transfer may originate from the difference of dimensions (3D vs 2D), or otherwise the difference of the character of the original gap, i.e., the Mott-Hubbard type for the titanates vs the charge-transfer type for the cuprates.<sup>27</sup>

## V. SUMMARY

To control the one-electron bandwidth ( $W$ ) and hence the relative strength of the electron correlation (as measured by  $\tilde{U} = U/W$ ), we have synthesized a series of the Mott-Hubbard insulators La<sub>x</sub>Y<sub>1-x</sub>TiO<sub>3</sub>. By measurements of the optical spectra, the Mott-Hubbard gap ( $E_g$ ) was observed to increase from 0.2 eV up to 1.2 eV with an increase of Y concentration. The relative gap magnitude  $\tilde{E}_g$  ( $= E_g/W$ ) was deduced as a function of the correlation strength  $\tilde{U}$ . The critical value,  $\tilde{U}_c$ , for the

hypothetical metal-insulator (Mott) transition was estimated precisely from the extrapolation procedure. The result indicated that the value of  $\eta$  ( $= \bar{U}/\bar{U}_c - 1$ ) ranges from 0.02 (LaTiO<sub>3</sub>) up to 0.22 (YTiO<sub>3</sub>).

The change of the gap spectra with hole doping was investigated for slightly oxygen-off-stoichiometric LaTiO<sub>3+ $\delta$ /2</sub> and the results were compared with the case of Y<sub>1-x</sub>Ca<sub>x</sub>TiO<sub>3</sub>, with stronger electron correlation. The spectral weight transfer from the Mott-Hubbard gap transition to the inner-gap excitations was observed to be similar to the case of the other hole-doped correlated insulators. The rate of the spectral weight transfer versus

the nominal hole-concentration is larger for the doped LaTiO<sub>3</sub> system than for the doped YTiO<sub>3</sub> system, which is perhaps relevant to the correlation strength (or  $\eta$  value) of the respective parent insulators.

#### ACKNOWLEDGMENTS

We are grateful to M. Imada and N. Nagaosa for enlightening discussion. The present work was supported by a Grant-In-Aid for Scientific Research from the Ministry of Education, Science, and Culture, Japan.

- <sup>1</sup> Y. Tokura, Jpn. J. Appl. Phys. **32**, 209 (1993).
- <sup>2</sup> J. B. Torrance, P. Lacorre, A. I. Nazzari, E. J. Ansaldo, and Ch. Niedermayer, Phys. Rev. B **45**, 8209 (1992).
- <sup>3</sup> D. A. Crandles, T. Timusk, J. D. Garrett, and J. E. Greedan, Physica C **201**, 407 (1992).
- <sup>4</sup> F. Lichtenberg, D. Widmer, J. G. Bednorz, T. Williams, and A. Reller, Z. Phys. B **82**, 211 (1991).
- <sup>5</sup> Y. Tokura, Y. Taguchi, Y. Okada, T. Arima, K. Kumagai, and Y. Iye, Phys. Rev. Lett. **70**, 2126 (1993).
- <sup>6</sup> Y. Fujishima, Y. Tokura, T. Arima, and S. Uchida, Phys. Rev. B **46**, 11 167 (1992).
- <sup>7</sup> Y. Taguchi, Y. Tokura, T. Arima, and F. Inaba, Phys. Rev. B **48**, 511 (1993).
- <sup>8</sup> Y. Okada, T. Arima, Y. Tokura, C. Murayama, and N. Môri, Phys. Rev. B **48**, 9677 (1993).
- <sup>9</sup> D. A. Crandles, T. Timusk, J. D. Garrett, and J. E. Greedan, Phys. Rev. B **49**, 16 207 (1994).
- <sup>10</sup> D. A. MacLean, Hok-Nam Ng, and J. E. Greedan, J. Solid State Chem. **30**, 35 (1979).
- <sup>11</sup> W. A. Harrison, *Electronic Structure and Properties of Solids* (Freeman, San Francisco, 1980).
- <sup>12</sup> J. P. Goral, J. E. Greedan, and D. A. Maclean, J. Solid State Chem. **43**, 244 (1982).
- <sup>13</sup> L. M. Roth, Phys. Rev. **149**, 306 (1966).
- <sup>14</sup> S. Inagaki, J. Phys. Soc. Jpn. **39**, 596 (1975).
- <sup>15</sup> M. Cyrot and C. Lyon-Caen, J. Phys. **36**, 253 (1975).
- <sup>16</sup> C. W. Turner and J. E. Greedan, J. Solid State Chem. **34**, 207 (1980).
- <sup>17</sup> J. E. Greedan, J. Less-Common Met. **111**, 335 (1985).
- <sup>18</sup> T. Arima, Y. Tokura, and J. B. Torrance, Phys. Rev. B **48**, 17 006 (1993).
- <sup>19</sup> T. Uozumi, K. Okada, and A. Kotani, J. Phys. Soc. Jpn. **62**, 2595 (1993).
- <sup>20</sup> W. F. Brinkman and T. M. Rice, Phys. Rev. B **2**, 4302 (1970).
- <sup>21</sup> S. Uchida, T. Ido, H. Takagi, T. Arima, Y. Tokura, and S. Tajima, Phys. Rev. B **43**, 7942 (1991).
- <sup>22</sup> S. L. Cooper, G. A. Thomas, J. Orenstein, D. H. Rapkine, A. J. Mills, S.-W. Cheong, A. S. Cooper, and Z. Fisk, Phys. Rev. B **41**, 11 605 (1990).
- <sup>23</sup> T. Arima, Y. Tokura, and S. Uchida, Phys. Rev. B **48**, 6597 (1993).
- <sup>24</sup> M. Kasuya, Y. Tokura, T. Arima, H. Eisaki, and S. Uchida, Phys. Rev. B **47**, 6197 (1993).
- <sup>25</sup> I. Terasaki, T. Nakahashi, S. Takebayashi, and K. Uchinokura, Phys. Rev. B **43**, 551 (1991).
- <sup>26</sup> E. Dagotto, A. Moreo, F. Ortolani, D. Poilblanc, and J. Riera, Phys. Rev. B **45**, 10 741 (1992).
- <sup>27</sup> J. Zaanen, G. A. Sawatzky, and J. W. Allen, Phys. Rev. Lett. **55**, 418 (1985).